

A demonstration of rotating sound waves in free space and the transfer of their angular momentum to matter

Arturo O. Santillán

Centro de Ciencias Aplicadas y Desarrollo Tecnológico, Universidad Nacional Autónoma de México, Apdo. Postal 70-186, 04510 Mexico D. F., Mexico

Karen Volke-Sepúlveda^{a)}

Instituto de Física, Universidad Nacional Autónoma de México, Apdo. Postal 20-364, 01000 Mexico D.F., Mexico

(Received 16 April 2008; accepted 5 December 2008)

We describe an apparatus for generating rotating sound waves in free space by superimposing two orthogonal standing modes with a quarter wave phase lag. The creation of a standing wave from the superposition of two counter-rotating waves is also possible with the same apparatus. The experiment permits direct measurement of both the amplitude and phase structure of the sound waves. A demonstration of angular momentum transfer from rotating acoustic waves to matter in free field is also described. © 2009 American Association of Physics Teachers.

[DOI: 10.1119/1.3056580]

I. INTRODUCTION

The concept of rotating waves was raised to the same level of traveling and standing waves by Ceperley in 1992.¹ He proposed an experiment to observe rotating waves propagating in circles on the surface of water inside a cylindrical container. In the same year a detailed analysis of rotating waves of light in the form of Laguerre–Gaussian laser modes was presented.² These modes can be generated with a continuous laser by using a mode converter, and their phase structure can be analyzed with an interferometer.³ There are also simpler ways of generating Laguerre–Gaussian modes by means of computer generated holograms.⁴ Rotating waves are usually discussed in an abstract context in undergraduate courses of quantum mechanics.¹ This context does not help to establish a clear relation between matter waves and other familiar wave fields such as light, sound, and surface waves in liquids.

One of the most interesting properties of rotating waves is that they carry angular momentum that can be transferred to matter, just as the linear momentum of traveling waves. This property has attracted significant attention due to the possibility of controlling the rotation of microscopic particles trapped with optical tweezers.^{5–8} Although these experiments are too complicated to perform in nonspecialized laboratories, rotation of matter produced by sound waves offers an interesting alternative way to observe the same phenomenon with macroscopic objects.^{9,10} For example, although the phase structure of light waves can be analyzed only indirectly by interference experiments, the phase of sound waves can be measured directly with respect to a reference signal. In contrast, the intensity distribution of light can be directly observed, and the intensity distribution of an acoustic field has to be determined by simultaneous measurements of the sound pressure by means of two microphones. In that sense, optical, and acoustical demonstrations complement and reinforce each other.

In this paper we describe how to generate and analyze rotating sound waves in free space. The same setup can be used to demonstrate angular momentum transfer from sound waves to matter and perform quantitative measurements. Although rotating sound waves have been produced and used for setting matter into rotation inside a cavity,^{11,12} the free

space conditions provided by our apparatus allow direct measurements of the acoustic field in amplitude and phase. Although the focus of our paper is on demonstrations with sound waves, we will discuss waves more generally to emphasize aspects common to all wave phenomena, regardless of their longitudinal or transverse nature.

II. ROTATING AND STANDING WAVES

We consider monochromatic waves propagating in a linear medium, characterized by their angular frequency ω , wavelength λ , and the propagation or phase velocity $v = \omega/k$, where $k = 2\pi/\lambda$ is the wave number and $T = 2\pi/\omega$ is the period. Monochromatic waves exhibit no dispersion and, when propagating in a linear medium, have a constant velocity which does not depend on their amplitude. All these conditions can be fulfilled for sound and continuous laser light waves propagating in air.

For propagating waves, characterized by a phase of the form $[vt \pm f(x, y, z)]$, the function $f(x, y, z)$ is associated with the shape and propagation direction of the wave fronts. A wave function of the form $\Psi(x, y, z, t) = A(\rho)\cos(\omega t - \varphi)$, where $\varphi = \arctan(y/x)$ and $\rho = (x^2 + y^2)^{1/2}$, represents a wave that travels along the positive φ direction, that is, a rotating wave. The amplitude $A(\rho)$ of the wave depends on the radial coordinate because the value of the phase is undefined at $\rho = 0$. Therefore, it is necessary that $A = 0$ at that point. The most general case of a purely rotating wave is described by

$$\Psi_R(x, y, t) = A_m(\rho)\cos(\omega t \mp m\varphi), \quad (1)$$

where $m \neq 0$ is a positive integer. In this case there are m wave fronts corresponding to semi-infinite planes that rotate in circles around the z axis as time evolves. The amplitude is labeled by m because the radial dependence is linked to the angular dependence via the solutions of the wave equation. Close to the rotation axis, there is always a leading term of the form ρ^m in the radial dependence.

If a wave is traveling forward at the same time that it rotates, the wave is known as helical, and its wave function has the form $\Psi_H = A_m(\rho, z)\cos(\omega t - kz \mp m\varphi)$. The effect on the wave fronts of the z dependence is to twist the semi-infinite planes like corkscrews. The wave fronts correspond

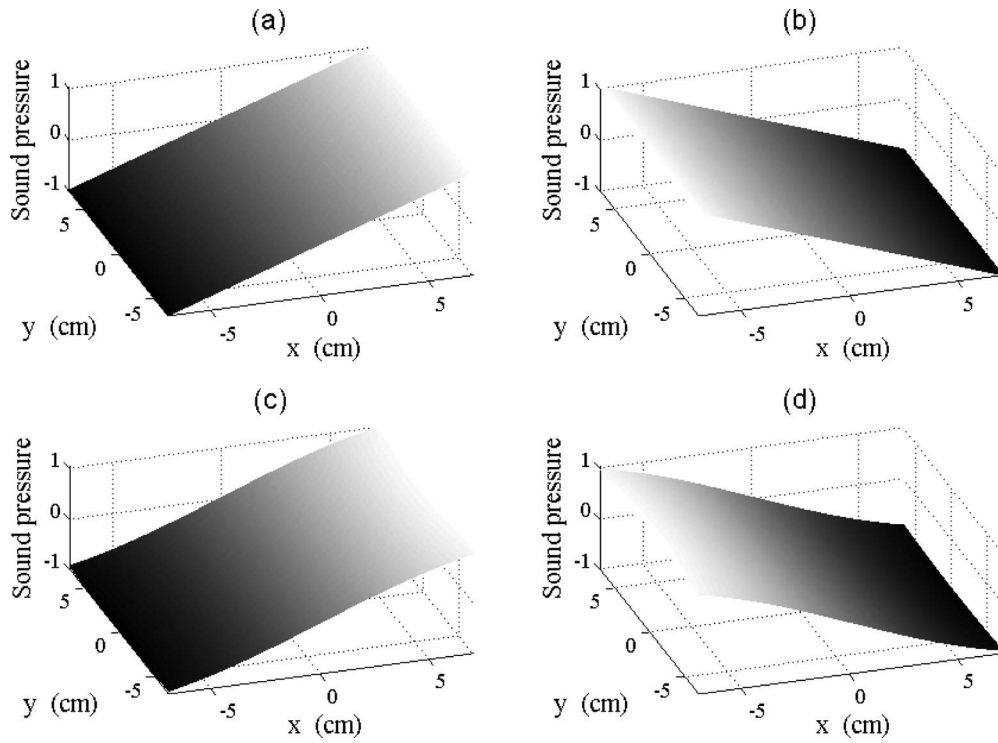


Fig. 1. (a) Spatial distribution at $t=0$ of the normalized sound pressure for the ideal wave $\Psi_S = \rho \cos \varphi \cos \omega t$. (b) The same for $t=T/2$, where T is the period. (c) Graphs of the instantaneous value of the sound pressure at the plane $z=\lambda$ for a wave generated by the superposition of two simple sources emitting half a wavelength out of phase at the time $t=0$. (d) The same for $t=T/2$. The simple sources were assumed to be at $x = \pm a$, with $a=18.5$ cm, and $f=1300$ Hz.

to m intertwined helices,³ each one completing a twist in a distance of $m\lambda$ and rotating with constant angular velocity ω/m .

Rotating and helical waves are also called wave vortices because their distributions of energy flux and linear momentum density in the transverse plane resemble the velocity field of a vortex fluid. There are, for instance, optical^{13,14} and acoustical vortices.^{15,16} In this context m is known as the topological charge or the order of the vortex.^{14,15}

The superposition of two counter-rotating waves of the same amplitude and frequency gives rise to standing waves of the form

$$\Psi_S(x, y, t) = 2A_m(\rho) \cos m\varphi \cos \omega t. \quad (2)$$

In this case there are $2m$ nodes defined by the condition $m\varphi = (2n-1)\pi/2$, where n is an integer with values from 1 to $2m$.

The interference of two orthogonal standing waves oscillating about their nodal surfaces with a relative phase shift of $\mp \pi/2$ produces a rotating wave

$$\begin{aligned} \Psi_R(x, y, t) &= A_m(\rho) [\cos m\varphi \cos \omega t \\ &\quad + \sin m\varphi \cos(\omega t \mp \pi/2)] \\ &= A_m(\rho) \cos(\omega t \mp m\varphi). \end{aligned} \quad (3)$$

The negative sign of the phase shift (a phase delay) gives rise to a wave rotating in the counterclockwise direction, whereas a positive phase shift results in a clockwise rotation. It is common to represent a wave vortex of order m in complex notation as^{13,14} $(x \mp iy)^m \exp(i\omega t) = \rho^m \exp[i(\omega t \mp m\varphi)]$. This expression is appropriate for small values of ρ regardless of the form of the function $A_m(\rho)$.

III. HOW TO GENERATE ACOUSTIC ROTATING WAVES

Our procedure for producing rotating sound waves is based on Eq. (3). We generated two orthogonal standing waves and then superimposed them with the necessary phase shift. The simplest case of the standing wave described by Eq. (2) corresponds to $m=1$. In free space a reasonable approximation to this function can be generated with a pair of simple sound sources of angular frequency ω located at opposite points around a circumference of radius a in a horizontal plane, for instance, at the points $x = \pm a$. Each source emits spherical waves.¹⁷ If the two sources have a relative phase shift of π , nodal surfaces will be formed in the semi-infinite planes defined by $\varphi = \pi/2$ and $\varphi = 3\pi/2$, which join together in a single plane, $x=0$. For comparative purposes, Figs. 1(a) and 1(b) illustrate the function $\Psi_S = \rho \cos \varphi \cos \omega t$ at time $t=0$ and $t=T/2$ respectively, and Figs. 1(c) and 1(d) show snapshots of the wave field produced by the two simple sources, each source radiating spherical waves at $t=0$ and $t=T/2$ in the plane $z=\lambda$. For the graphs in Fig. 1 we used $a=18.5$ cm, and frequency $f=1300$ Hz. Similarly, an approximation to the orthogonal standing wave $\Phi_S = \rho \sin \varphi \cos \omega t$ can be produced by placing a second pair of sources at the points $y = \pm a$, emitting with a relative phase of π .

The superposition of a pair of orthogonal standing waves will produce a rotating wave as described by Eq. (3). For this purpose the relative phases between the four sources can be set, for instance, in the way shown in Fig. 2. This configuration of simple sources gives a good approximation to the desired rotating wave in a region close to the z axis; inter-

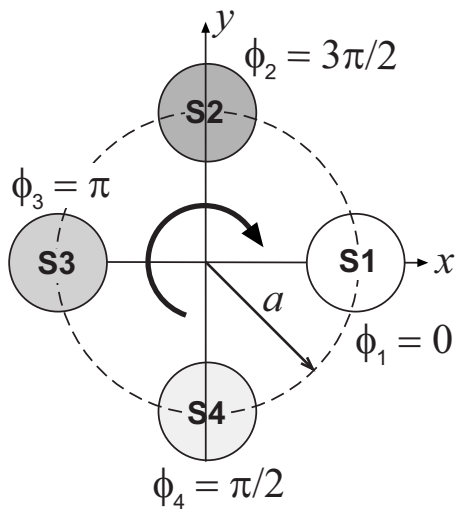


Fig. 2. Distribution of four simple sources and their relative phases to produce a rotating sound wave. The gray scale of the sources is related to the value of their relative phases. White corresponds to a phase of zero (S1), and the darkest gray corresponds to a relative phase of $3\pi/2$ (S2). The phase increases in the clockwise direction, as indicated by the circular arrow, but the wave rotates in the counterclockwise direction, according to the expression $\exp[i(\omega t - \varphi)]$. The direction of the rotation can be inverted by interchanging the relative phase of sources S2 and S4.

ested readers can find the details in Ref. 16. An additional exercise would be to superimpose the orthogonal standing waves with a different phase lag between them, $[\cos \varphi \cos \omega t + \sin \varphi \cos(\omega t + \delta)]$. In this way it can be verified that the pure rotating wave is produced only when the phase shift is $\delta = \pm \pi/2$. Note that when the phase lag is zero, we obtain a standing wave whose nodal plane is rotated by 45° with respect to the nodes of the superimposed standing waves because $\cos \varphi + \sin \varphi = \cos(\varphi + \pi/4)$.

The generation of a standing wave from the superposition of two counter-rotating waves can be demonstrated experimentally. For this purpose it is necessary to use a minimum of eight sources evenly distributed around a circumference of radius a because we need four sources to generate each rotating wave. An example of a suitable configuration of the relative phases of the eight sources is indicated in Fig. 3(a). With the same setup of eight sources it is also possible to generate an acoustical vortex of second order,¹⁶ or topological charge $m=2$. For the latter case an appropriate configuration of relative phases is shown in Fig. 3(b).

IV. EXPERIMENT

The experimental apparatus is depicted in Fig. 4(a). We used a plate of plywood as a baffle, 70 cm on a side and 1.2 cm thick. To connect the sound sources we made eight circular holes distributed uniformly around a circumference of radius $a=18.5$ cm in the wooden plate. We used drivers for horn loudspeakers (Eminence PSD-2002) as sound sources. Each driver was coupled to the baffle through one of the holes by using a PVC tube with inner diameter $D=3.5$ cm and length $L=6$ cm. The size of the holes in the baffle fit the diameter of the tube. We sealed the joints of the ends of each tube with the drivers and with the baffle by using modeling clay. In this way the sound generated with each driver was radiated through the opening of the tube. The length of the tubes determined a resonance frequency in

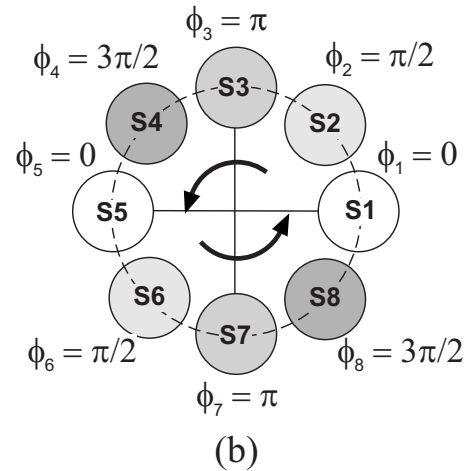
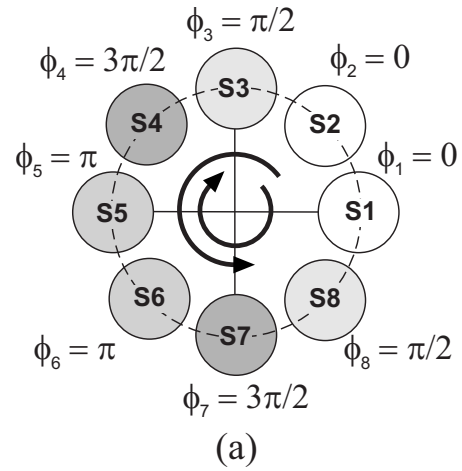


Fig. 3. (a) Relative phase and distribution of eight simple sources to produce a standing wave from the superposition of two counter-rotating waves. Sources S1, S3, S5, and S7 generate a wave rotating in the clockwise direction, and sources S2, S4, S6, and S8 produce a wave rotating in the counterclockwise direction. The gray scale of the sources in the figure is related to their relative phases. (b) Relative phase and distribution of the eight sources for producing a second-order acoustical vortex. For this configuration the phase increases in the counterclockwise direction as indicated by the circular arrows, but the wave rotates in the clockwise direction according to the expression $\exp[i(\omega t + 2\varphi)]$. In this case, the sources S1, S3, S5, and S7 produce a standing mode of the form $[\cos 2\varphi \cos \omega t]$, and the sources S2, S4, S6, and S8 generate a mode of the form $[\sin 2\varphi \cos(\omega t + \pi/2)]$. The superposition of the two standing waves gives rise to the rotating wave.

the driver-tube system of 1300 Hz ($\lambda \approx 26.3$ cm). The inner diameter of each tube was much smaller than the corresponding wavelength, and the air at the end of the opening behaved as an air piston. Therefore, each opening in the baffle radiated sound as a simple source at that frequency, producing spherical waves. In the following we use the term simple source to refer to any of those openings.

Each driver was connected to an independent channel of an audio amplifier, in our case two channels per amplifier. The amplifiers were fed by using eight channels of an external sound card (Echo, Layla 24) controlled by a personal computer [see Fig. 4(b)].

We measured the sound field with an omnidirectional precision microphone (B&K 4134) connected to a two-channel FFT signal analyzer (B&K 2034). An alternative is to use an oscilloscope instead of the analyzer and a bandpass filter to

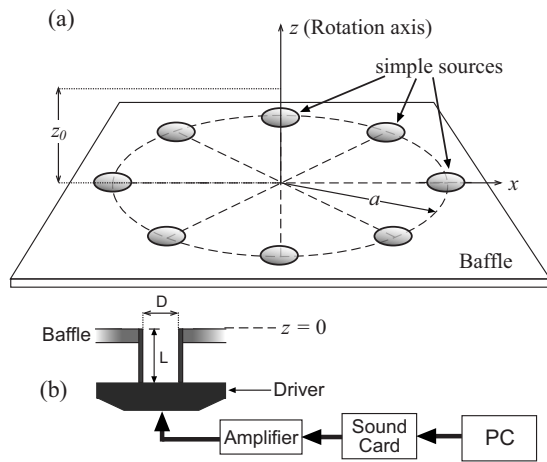


Fig. 4. (a) Apparatus for the generation of rotating and standing acoustic waves. A plywood baffle holds eight simple sources distributed around a circumference of radius a . The horizontal plane of the baffle is set as the x - y plane and the z axis is the vertical axis passing through the center of the circumference. (b) Diagram illustrating the system for the reproduction of the sound wave for one driver. Each driver is coupled to the baffle through a hole by means of a PVC tube of diameter $D=3.5$ cm and length $L=6$ cm, and is connected to an independent channel of an audio amplifier. The amplifiers are fed by using eight channels of an external sound card controlled with a personal computer.

reduce the background noise received by the microphone. The signal from the first output channel of the sound card was connected, after being amplified, to input channel 1 of the analyzer and used as the reference signal (see Fig. 5). In this way, the phase of the generated sound field was measured with respect to that signal. For that purpose the transfer function between the signal from the microphone and the reference signal was determined in the analyzer. The transfer function in this case is the ratio of the Fourier transform of the signal from the microphone (in channel 2 of the analyzer) to the Fourier transform of the reference signal (in channel 1). The system was operated continuously during the measurements to achieve a steady state. The average of five samples of the transfer function was sufficient to give a well defined value of the phase at the frequency of interest. The amplitude was also determined by the average of five spectra of the signal from the microphone. The time dependence set in the analyzer has the form $\exp(i\omega t)$, which is consistent with Eq. (1).

To have precise control of the phase and amplitude of the sound radiated by each simple source it is necessary to characterize each of the eight reproduction chains individually. A reproduction chain is the system composed of all the elements for the reproduction of sound, from the sound card to one of the simple sources. For the characterization of the reproduction chains we placed the microphone 4 cm over the baffle along the z axis. Because each of the simple sources was equidistant from the microphone at that position, each should generate the same amplitude and relative phase on the microphone if they are fed with the same signal. Undesirable differences in both amplitude and phase were compensated when the eight output signals were generated. These eight signals, including the phase differences, were created by means of a MATLAB program (available upon request). In this way, *wav* files were first generated, and they were reproduced by using audio software.¹⁸

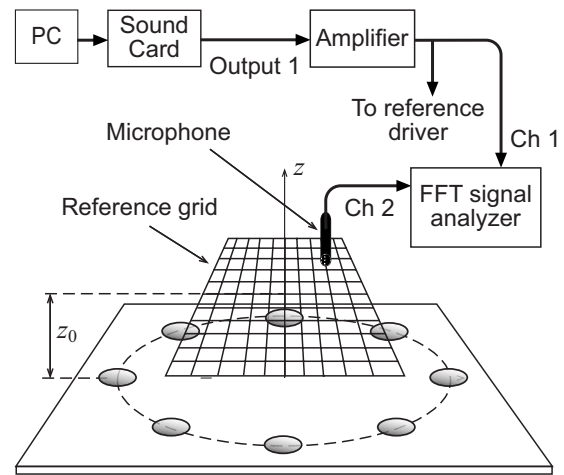


Fig. 5. System used to measure the sound pressure. A microphone was placed at specific positions indicated by a grid on the plane $z=z_0$. The signal from the microphone was connected to input channel 2 of a FFT analyzer. Output signal 1 of the sound card was fed to the first driver and was also connected to input channel 1 of the FFT analyzer to be used as the reference signal for the measurements of the phase.

The experiment was done inside a carpeted room with dimensions of $6\text{ m} \times 6\text{ m} \times 2.5\text{ m}$. The system with the drivers and the baffle was placed on a table in the center of the room. To minimize the effect of sound reflections from the walls and other surfaces into the region of interest around the baffle, we outfitted the room with rubber foam. We hung from the ceiling a block with a square area, 1.5 m on a side and 10 cm thick, at about 1 m over the baffle. We also placed four blocks, 1 m long, 40 cm high, and approximately 20 cm thick around the baffle, one block per side, and arranged 12 more of those blocks vertically in each corner of the room and along the walls.

The sound pressure field we generated in this way can be characterized by point measurements over a square grid in a transverse plane $z=z_0$ (in our case $z_0=4$ cm). We fabricated a grid with nylon threads tied to a square frame made of an aluminum tube (diameter <0.5 cm) in the two orthogonal directions (see Fig. 5). The measurement points (x_j, y_j) were at the intersections of the orthogonal threads, corresponding to the vertices of squares with 1 cm on a side. The conditions $-7\text{ cm} \leq x_j \leq 7\text{ cm}$ and $-7\text{ cm} \leq y_j \leq 7\text{ cm}$ define the measurement region. The microphone was manually positioned at the points of the grid, giving a total of 225 individual measurements per field. Although 225 is a large number of measurements, it took only about 2 h. This process can be simplified by considering a smaller measurement region or by using a positioning system for the microphone.

The results of the measurements for the root-mean-square (rms) amplitude and the phase of the rotating wave are shown in Fig. 6. We see that the amplitude of the sound pressure is independent of the azimuthal angle and that there is a minimum on the z axis. The value of the amplitude at the minimum differs from zero due mainly to the background noise. The graph of the phase has a helical shape because its value increases linearly from 0 to 2π along a circumference around the z axis. According to the experimental results, this sound field corresponds to a first-order acoustical vortex.¹⁶

We also used all eight drivers to produce a standing wave as the superposition of two counter-rotating waves. The mea-

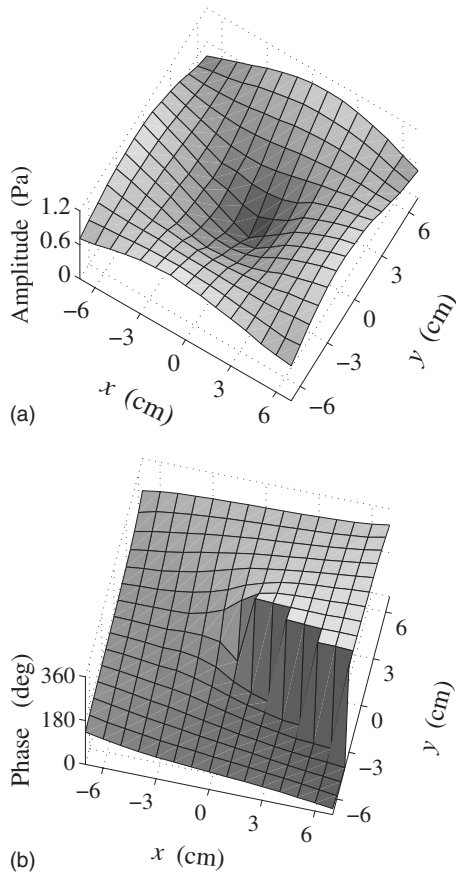


Fig. 6. Measurements of (a) the rms amplitude and (b) the relative phase of a first-order vortex or rotating wave. This acoustic field is generated with the configuration of simple sources illustrated in Fig. 2.

sured rms amplitude and phase are shown in Fig. 7. As expected, a nodal line appears, and there is a phase difference of 180° in the sound pressure on one side of the nodal line with respect to the other.

Finally, we generated a second-order acoustical vortex with the same experimental apparatus. As explained, this vortex is a rotating wave corresponding to $m = \pm 2$ in Eq. (3). All eight loudspeakers were driven with the same amplitude, with each one having a phase lag of $\pi/2$ with respect to its neighbor around the circumference,¹⁶ as shown in Fig. 3(b). The rms amplitude and the phase of the synthesized second-order vortex are shown in Fig. 8. The sound pressure amplitude has a minimum value at the center of the vortex and varies as ρ^2 . We can also see that there are two cycles in which the phase increases from 0 to 2π along a closed contour around the z axis.

To verify how much the sound field deteriorates due to reflections, we performed the same experiment inside an anechoic chamber. The results of these measurements look almost the same as those of Figs. 6–8, showing that the effect of reflections can be neglected in the region of interest.

V. ANGULAR MOMENTUM OF ROTATING WAVES

The angular momentum of light has been widely discussed, especially over the last two decades, when it was recognized that there are two different contributions.² A circularly polarized light wave carries angular momentum due

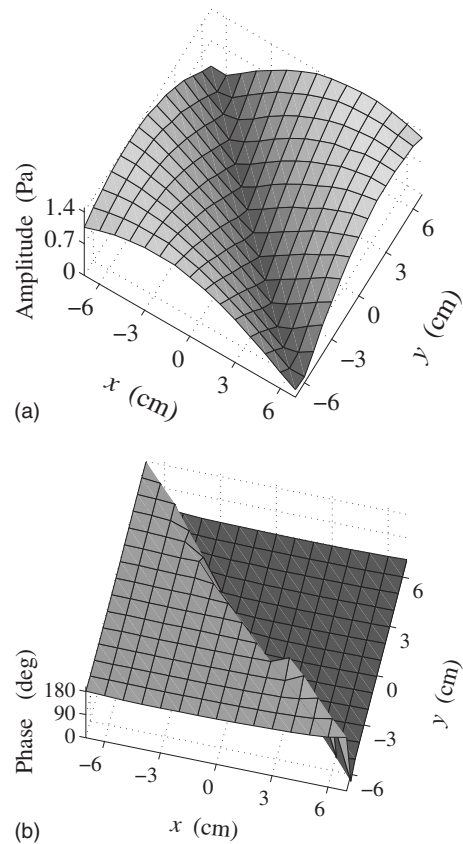


Fig. 7. Experimental results of the (a) rms amplitude and (b) phase of a standing wave generated by the superposition of two counter-rotating waves. This acoustic field is generated by the configuration of simple sources shown in Fig. 3(a).

to the rotation of the electric and magnetic fields.¹⁹ This is the spin contribution. In contrast, helical waves in optics, such as Laguerre–Gaussian^{2,3} and high order Bessel beams^{7,20} possess orbital angular momentum due to their rotating phase distribution. Both spin and orbital angular momentum have been transferred to matter in experiments with optically trapped microparticles of different kinds.^{5–8} The transfer of angular momentum from a wave field to matter has exciting applications, for example, in the development of light driven micromachines.²¹ A classical calculation of the z component of the angular momentum density of a helical wave of light gives rise to² $L_z = (\pm m + \sigma)\epsilon/\omega$, where ϵ represents the total energy density of the electromagnetic field, and σ equals 1, 0, or -1 if the polarization state of the field is left-handed circular, linear, or right-handed circular, respectively. The plus (minus) sign represents waves rotating in the counterclockwise (clockwise) direction. If we consider the energy per photon, $\epsilon = \hbar\omega$, we can associate an angular momentum per photon along the z axis² of $L_z = (\pm m + \sigma)\hbar$. The orbital angular momentum contribution, $\pm m\hbar$, reminds us of the z component of the orbital angular momentum of the electron moving around the nucleus in the hydrogen atom.

Because acoustic fields are longitudinal waves, they cannot have spin. However, they can possess orbital angular momentum if they have a rotating phase distribution as in the cases we have described. Recent experiments have shown that the angular momentum from rotating acoustic waves can

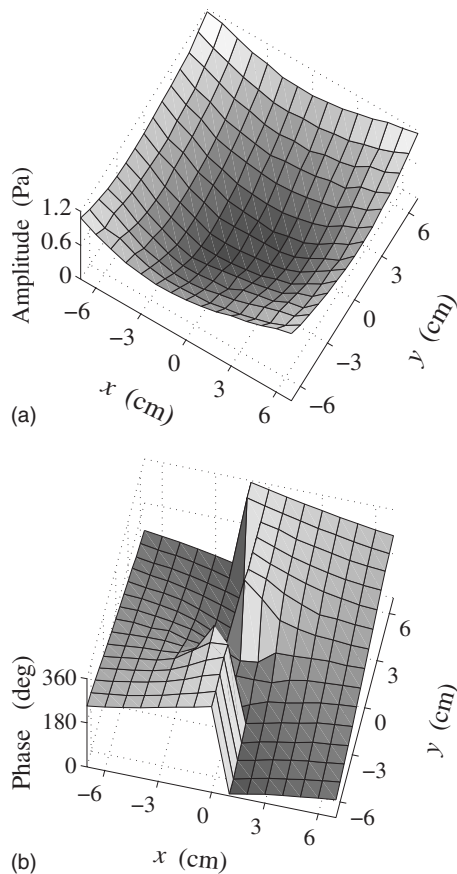


Fig. 8. Measurements of (a) the rms amplitude and (b) the phase of a second order ($m=2$) rotating wave. In this case there are two cycles around the circumference in which the phase increases linearly from 0 to 2π . This acoustic field is generated by the configuration of simple sources illustrated in Fig. 3(b).

also be transferred to matter.^{16,21} The z component of the angular momentum density for a sound wave rotating about this axis gives¹⁶ $L_z = \pm (m/\omega)p^2/(\rho_0 v^2)$, where $p^2/(\rho_0 v^2)$ is twice the acoustic potential energy density (p is the sound pressure, ρ_0 is the mean density of the propagation medium, and v is the sound speed). If the total energy density ε is equally distributed between the potential and kinetic contributions, we can write the angular momentum as $L_z = \pm (m/\omega)\varepsilon$, which is the same expression as for waves in optics and quantum mechanics, and is also the same expression found by Ceperley for the angular momentum of rotating waves on the water surface of a cylindrical container.¹ It is a general result for all waves carrying angular momentum, regardless of the nature of the waves, transverse or longitudinal.

It is possible to demonstrate the angular momentum transfer from sound waves to matter with the apparatus described in Sec. IV. Quantitative measurements of the acoustical torque can be done by implementing a torsion pendulum with a disk hanging over the baffle, perfectly aligned with the rotation axis of the sound field.^{16,22}

To make a qualitative, simpler, and equally illustrative demonstration we made a hollow acrylic cylinder, 2.4 cm in outer diameter and 2.2 cm high, with a small on-axis hole through one of the circular surfaces (see Fig. 9). Because the mechanism of angular momentum transfer in this case is absorption, it is necessary to cover the external surface of the

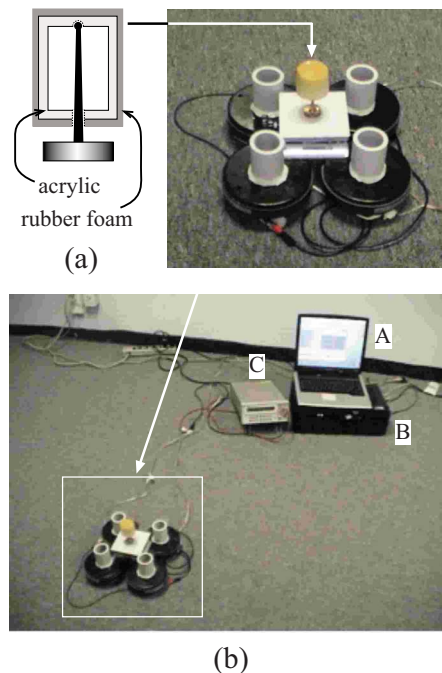


Fig. 9. (a) The experiment for demonstrating the angular momentum transfer from rotating acoustical waves to a cylinder covered by sound-absorptive rubber foam. Four loudspeakers are shown surrounding a base with the cylinder. The inset is a schematic diagram of the cylinder on its base. (b) Picture of the entire experimental setup, including the controlling computer A, the amplifier B, the multimeter C, and the part of the setup shown in (a).

cylinder with a layer of sound-absorptive rubber foam (approximately 1 cm thick in our case). We placed the cylinder on a base with a vertical needle by introducing the needle through the hole in the bottom surface of the cylinder. The needle must be perfectly aligned with the rotation axis of the acoustic field, as illustrated in Fig. 9(a). To keep the contact point between the needle and the cylinder on axis, we made a very small cavity at the center of the inner upper surface of the cylinder. Reducing the friction between the needle and the cylinder at the contact point, allows freer rotation.

Although the experimental apparatus described in Sec. IV can be used for this experiment, the sound pressure levels required might be high because the sources are relatively far from the rotation axis. Instead, we used only four drivers without the baffle, but with the PVC tubes attached to them to have the same resonance frequency of 1300 Hz in the driver-tube system. In this way, we were able to place the sound sources much closer to the cylinder and optimize the acoustic torque [Fig. 9(a)]. As a further simplification, each pair of opposite drivers were connected, but with inverted polarization of the connections to produce a π phase difference between the sound waves generated by the two drivers of each pair. In this way, only two output signals are needed with a phase lag of $\pi/2$ between them, one for each pair of sources. In our case the two drivers in each set were connected in parallel (a series or a parallel connection depends on the electric impedance that the amplifier can handle). The signals can be generated in stereo format, which allows their reproduction through the internal sound card of a computer [Fig. 9(b)]. The output signals are passed to an audio amplifier and fed to the two pairs of drivers.

The onset of the rotation was observed when the input voltage to the drivers was approximately $V_{\text{rms}}=8$ V, which

produced a rms electrical current of about 0.3 A in each transducer.²³ The rms current should be smaller than 1 A to avoid damage to the drivers. The sound pressure as measured with only one driver excited with $V_{\text{rms}}=8$ V was approximately 115 dB (referred to 20 μPa) at approximately 30 cm from the opening of the tube.

As explained in Sec. II, the rotation direction can be set in either direction depending on the sign of the $\pi/2$ phase shift between the two pairs of sources. Note that the higher the absorption of the sound-absorptive material, the easier the object rotates. We measured the absorption coefficient of the rubber foam by means of an impedance tube, giving a value of 0.066 at the frequency of 1300 Hz. The object should be large enough to cover an area where the amplitude of the rotating acoustic wave is significant, but it should remain as light as possible, with a small moment of inertia.

This experiment is noisy because the sound pressure required to produce rotations of a material object might be considerably higher than the one required for the simple generation and characterization of a particular sound field (see Sec. IV). It is important to ensure that everyone inside the room uses hearing protectors, the desired object is made of light materials, covered with very absorptive rubber foam, and with a diameter larger than approximately $\lambda/8$ so as to optimize the angular momentum transfer with the minimum possible sound level. Also the room should be isolated to avoid annoying people nearby.

VI. CONCLUSIONS

Rotating waves, characterized by angular momentum transport, can arise in different kinds of wave fields in nature. We have described an apparatus for generating and characterizing rotating sound waves in free space. In this case the rotating acoustic field is created by superimposing two orthogonal standing modes with a relative phase shift of $\pi/2$. Although the construction of the apparatus requires some effort, the required material is easy to obtain and inexpensive. The same apparatus can be used for the generation and characterization of different acoustic fields in free space. We also proposed an extension of the experiment for demonstrating that the angular momentum of rotating acoustic waves can be transferred to matter under free field conditions. In particular, it was shown that a rotating sound wave exerts a torque on an absorptive object aligned with the rotation axis of the wave.

ACKNOWLEDGMENTS

The authors acknowledge DGAPA-UNAM, Project No. IN-114407, and Anahi Flores-Perez for her valuable help in some of the experiments. They also thank the referees for their very useful comments and suggestions.

^{a)}Electronic mail: karen@fisica.unam.mx

- ¹P. H. Ceperley, "Rotating waves," *Am. J. Phys.* **60**, 938–942 (1992).
- ²L. Allen, M. W. Beijersbergen, R. J. C. Spreeuw, and J. P. Woerdman, "Orbital angular momentum of light and the transformation of Laguerre-Gaussian laser modes," *Phys. Rev. A* **45**, 8185–8189 (1992).
- ³M. Padgett, J. Arlt, N. Simpson, and L. Allen, "An experiment to observe the intensity and phase structure of Laguerre-Gaussian laser modes," *Am. J. Phys.* **64**, 77–82 (1996).
- ⁴E. J. Galvez, "Gaussian beams in the optics course," *Am. J. Phys.* **74**, 355–361 (2006).
- ⁵H. He, M. E. J. Friese, N. R. Heckenberg, and H. Rubinsztein-Dunlop, "Direct observation of transfer of angular momentum to absorptive particles from a laser beam with a phase singularity," *Phys. Rev. Lett.* **75**, 826–829 (1995).
- ⁶N. B. Simpson, K. Dholakia, L. Allen, and M. J. Padgett, "Mechanical equivalence of spin and orbital angular momentum of light: An optical spanner," *Opt. Lett.* **22**, 52–54 (1997).
- ⁷K. Volke-Sepúlveda, V. Garcés-Chávez, S. Chávez-Cerda, J. Arlt, and K. Dholakia, "Orbital angular momentum of a high-order Bessel light beam," *J. Opt. B: Quantum Semiclassical Opt.* **4**, S82–S89 (2002).
- ⁸V. Garcés-Chávez, D. McGloin, M. J. Padgett, W. Dultz, H. Schmitzer, and K. Dholakia, "Observation of the transfer of the local angular momentum density of a multi-ringed light beam to an optically trapped particle," *Phys. Rev. Lett.* **91**, 093602-1–4 (2003).
- ⁹A. Larraza, "A demonstration apparatus for an acoustic analog to the Casimir effect," *Am. J. Phys.* **67**, 1028–1030 (1999).
- ¹⁰B. Denardo and T. G. Simmons, "An acoustic radiometer," *Am. J. Phys.* **72**, 843–845 (2004).
- ¹¹T. G. Wang, H. Kanber, and I. Rudnick, "First-order torques and solid-body spinning velocities in intense sound fields," *Phys. Rev. Lett.* **38**, 128–130 (1977).
- ¹²C. P. Lee and T. G. Wang, "Near-boundary streaming around a small sphere due to two orthogonal standing waves," *J. Acoust. Soc. Am.* **85**, 1081–1088 (1989).
- ¹³G. Indebetow, "Optical vortices and their propagation," *J. Mod. Opt.* **40**, 73–87 (1993).
- ¹⁴M. V. Berry, "Much ado about nothing: Optical dislocation lines (phase singularities, zeros, vortices...)," in *Singular Optics*, SPIE Proceedings Vol. 3487, edited by M. S. Soskin (SPIE Optical Engineering, Bellingham, WA, 1998), pp. 1–5.
- ¹⁵J. L. Thomas and R. Marchiano, "Pseudo angular momentum and topological charge conservation for nonlinear acoustical vortices," *Phys. Rev. Lett.* **91**, 244302-1–4 (2003).
- ¹⁶K. Volke-Sepúlveda, A. O. Santillán, and R. R. Boulosa, "Transfer of angular momentum to matter from acoustical vortices in free space," *Phys. Rev. Lett.* **100**, 024302-1–4 (2008).
- ¹⁷L. E. Kinsler, A. R. Frey, A. B. Coppens, and J. V. Sanders, *Fundamental of Acoustics*, 4th ed. (Wiley, New York, 2000), p. 175.
- ¹⁸We used Cool Edit, which is now available as Adobe Audition. Other software options on Windows are Ableton Live and Tracktion.
- ¹⁹E. Hecht, *Optics*, 4th ed. (Addison-Wesley, San Francisco, CA, 2002), pp. 330–331.
- ²⁰S. Chávez-Cerda, G. S. McDonald, and G. H. C. New, "Nondiffracting beams: Travelling, standing, rotating and spiral waves," *Opt. Commun.* **123**, 225–233 (1996).
- ²¹H. Rubinsztein-Dunlop and M. Friese, "Light-driven micromachines," *Opt. Photonics News* **13**, 22–26 (2002).
- ²²K. D. Skeldon, C. Wilson, M. Edgar, and M. J. Padgett, "An acoustic spanner and its associated rotational Doppler shift," *New J. Phys.* **10**, 013018-1–9 (2008).
- ²³See EPAPS Document No. E-AJPIAS-77-005903 for a video file showing the rotation of a cylinder. For more information on EPAPS see <http://www.aip.org/pubservs/epaps.html>.